Intermolecular energy transfer in the presence of dispersing and absorbing media

Ho Trung Dung,* Ludwig Knöll, and Dirk-Gunnar Welsch
Theoretisch-Physikalisches Institut, Friedrich-Schiller-Universität Jena, Max-Wien-Platz 1, 07743 Jena, Germany
(Received 30 July 2001; published 1 April 2002)

By making use of the Green-function concept of quantization of the electromagnetic field in Kramers-Kronig consistent media, a rigorous quantum-mechanical derivation of the rate of intermolecular energy transfer in the presence of arbitrarily shaped, dispersing, and absorbing material bodies is given. Applications to bulk material, multislab planar structures, and microspheres are studied. It is shown that when the two molecules are near a planar interface, then surface-guided waves can strongly affect the energy transfer and essentially modify both the (Förster) short-range R^{-6} dependence of the transfer rate and the long-range R^{-2} dependence, which are typically observed in free space. In particular, enhancement (inhibition) of energy transfer can be accompanied by inhibition (enhancement) of donor decay. Results for four- and five-layered planar structures are given and compared with experimental results. Finally, the energy transfer between two molecules located at diametrically opposite positions outside a microsphere is briefly discussed.

DOI: 10.1103/PhysRevA.65.043813 PACS number(s): 42.50.Ct, 12.20.−m, 42.60.Da, 82.20.Rp

I. INTRODUCTION

Intermolecular energy transfer as a fundamental process in many biochemical and solid-state systems has been of increasing interest [1]. It is often distinguished between two cases, namely, (radiationless) short-range transfer (also called Förster transfer [2]) and (radiative) long-range transfer. In the former the distance R between donor and acceptor is small compared with the electronic-energy-transfer wavelength λ_A, $R/\lambda_A \ll 1$. The free-space transfer rate behaves as R^{-6}, which can be explained by the instantaneous (longitudinal) Coulomb interaction between the two molecules. In the latter the intermolecular distance substantially exceeds the transition wavelength, $R/\lambda_A \gg 1$. The observed R^{-2} dependence of the transfer rate can be regarded as being the result of emission and reabsorption of real (transverse) photons. It is worth noting that in a rigorous approach to the problem (e.g., within the framework of the multipolar formalism of QED [3,4]) the R^{-6} and R^{-2} distance dependences are limiting cases of a unified theory [5].

When the two molecules are near material bodies, then the electromagnetic field ''felt'' by them can be quite different from that in free space and the intermolecular energy transfer can change accordingly. The effect has attracted attention, because it offers the possibility of controlling the energy transfer, with regard to potential applications, e.g., in high-efficiency light-harvesting systems, optical networks, and quantum computing. Enhanced energy transfer between molecules randomly distributed within a single glycerol droplet (of about 10 μm diameter) [6] and within a polymer Fabry-Pérot microcavity [7] has been observed. Using monomolecular layers of donor and acceptor molecules (separated by distances of 10–20 nm) in planar microstructures, the dependence of short-range energy transfer on the local photon-mode density has been demonstrated [8].

Calculations of the energy-transfer rate have been performed in order to include the effect of bulk material [9], microspheres [10–13], and planar microcavities [14,15]. The quantum theory given in Ref. [9] is based on a microscopic model that allows for both dispersing and absorbing bulk material. In Refs. [10,11] the classical field generated by a donor dipole and felt by an acceptor dipole in the presence of a microsphere is substituted into the free-space Fermi's golden rule expression. A strictly quantum-mechanical treatment that starts from a mode decomposition of the electromagnetic field according to the Helmholtz equation of the macroscopic Maxwell equations is given in Refs. [12,14,15]. Unfortunately, the microscopic theory developed for bulk material [9] becomes quite cumbersome when boundaries are present, and studies based on the standard mode expansion [12,14,15] cannot incorporate material absorption.

In the present paper we give a rigorous derivation of the rate of intermolecular energy transfer in the presence of arbitrarily shaped, dispersing, and absorbing material bodies, starting from the quantized version of the macroscopic electromagnetic field. The quantization is based on the introduction of Langevin noise current and charge densities into the classical Maxwell equations, which can then be transferred to quantum theory, with the electromagnetic-field operators being expressed in terms of a continuous set of fundamental bosonic fields via the classical Green tensor (see [16,17] and references therein). In particular, we show that the minimal-coupling scheme and the multipolar-coupling scheme yield exactly the same form of the rate formula. It is worth noting that the formalism includes material absorption and dispersion in a consistent way, without restriction to a particular frequency domain, and applies to an arbitrary (inhomogeneous) medium configuration.

Here, we apply the theory to bulk material, multislab planar structures, and microspheres, with special emphasis on media of Drude-Lorentz type. In particular, we show that the energy transfer can be strongly modified, if the two molecules are sufficiently near an interface and surface-guided waves at the energy-transfer wavelength exist. Four- and five-layered planar structures are studied, and the results are

*On leave from the Institute of Physics, National Center for Sciences and Technology, 1 Mac Dinh Chi Street, District 1, Ho Chi Minh City, Vietnam.

compared with recent measurements [8]. Finally, the effect of surface-guided waves and whispering-gallery waves in the case of the molecules being near a microsphere is briefly discussed.

The paper is organized as follows. In Sec. II the basic-theoretical concept of electromagnetic-field quantization is outlined and the energy-transfer rate is derived. Section III is devoted to applications, with special emphasis on multislab planar structures, and concluding remarks are made in Sec. IV. Some explanatory calculations are given in the Appendix.

II. BASIC EQUATIONS

A. The Hamiltonian

Let us consider an ensemble of point charges, interacting with the quantized electromagnetic field in the presence of absorbing media. The minimal-coupling Hamiltonian in the Coulomb gauge reads [17,18]

$$\hat{H}=\int d^3\mathbf{r}\int_0^\infty d\omega\,\hbar\omega\,\hat{\mathbf{f}}^\dagger(\mathbf{r},\omega)\hat{\mathbf{f}}(\mathbf{r},\omega)+\sum_\alpha\frac{1}{2m_\alpha}\times[\hat{\mathbf{p}}_\alpha-q_\alpha\hat{\mathbf{A}}(\hat{\mathbf{r}}_\alpha)]^2+\frac{1}{2}\int d^3\mathbf{r}\hat{\rho}(\mathbf{r})\hat{\phi}(\mathbf{r})+\int d^3\mathbf{r}\hat{\rho}(\mathbf{r})\hat{\varphi}(\mathbf{r}),\tag{1}$$

where $\hat{\mathbf{r}}_\alpha$ is the position operator and $\hat{\mathbf{p}}_\alpha$ is the canonical momentum operator of the αth (nonrelativistic) particle of charge q_α and mass m_α. The first term of the Hamiltonian is the energy of the medium-assisted electromagnetic field, expressed in terms of bosonic vector fields $\hat{\mathbf{f}}(\mathbf{r},\omega)$ with commutation relations

$$[\hat{\mathbf{f}}_k(\mathbf{r},\omega),\hat{\mathbf{f}}^\dagger_{k'}(\mathbf{r}',\omega')]=\delta_{kk'}\delta(\mathbf{r}-\mathbf{r}')\,\delta(\omega-\omega'),\tag{2}$$

$$[\hat{\mathbf{f}}_k(\mathbf{r},\omega),\hat{\mathbf{f}}_{k'}(\mathbf{r}',\omega')]=0.\tag{3}$$

The second term is the kinetic energy of the charged particles and the third term is their Coulomb energy, where the corresponding scalar potential $\hat{\phi}(\mathbf{r})$ is given by

$$\hat{\phi}(\mathbf{r})=\int d^3\mathbf{r}'\frac{\hat{\rho}(\mathbf{r}')}{4\pi\varepsilon_0|\mathbf{r}-\mathbf{r}'|},\tag{4}$$

with

$$\hat{\rho}(\mathbf{r})=\sum_\alpha q_\alpha\delta(\mathbf{r}-\hat{\mathbf{r}}_\alpha)\tag{5}$$

being the charge density of the particles and ε_0 is the vacuum dielectric permittivity. The last term is the Coulomb energy of interaction of the particles with the medium.

The scalar potential $\hat{\varphi}(\mathbf{r})$ and the vector potential $\hat{\mathbf{A}}(\mathbf{r})$ of the medium-assisted electromagnetic field are given by

$$-\boldsymbol{\nabla}\hat{\varphi}(\mathbf{r})=\int_0^\infty d\omega\,\underline{\widehat{\mathbf{E}}}^{\parallel}(\mathbf{r},\omega)+\text{H.c.},\tag{6}$$

$$\hat{\mathbf{A}}(\mathbf{r})=\int_0^\infty d\omega(i\omega)^{-1}\underline{\widehat{\mathbf{E}}}^{\perp}(\mathbf{r},\omega)+\text{H.c.},\tag{7}$$

where

$$\underline{\widehat{\mathbf{E}}}^{\perp(\parallel)}(\mathbf{r},\omega)=\int d^3\mathbf{r}'\,\boldsymbol{\delta}^{\perp(\parallel)}(\mathbf{r}-\mathbf{r}')\underline{\widehat{\mathbf{E}}}(\mathbf{r}',\omega),\tag{8}$$

with $\boldsymbol{\delta}^\perp(\mathbf{r})$ and $\boldsymbol{\delta}^\parallel(\mathbf{r})$ being the transverse and longitudinal dyadic δ functions, respectively, and

$$\underline{\widehat{\mathbf{E}}}(\mathbf{r},\omega)=i\sqrt{\frac{\hbar}{\pi\varepsilon_0}}\frac{\omega^2}{c^2}\int d^3\mathbf{r}'\sqrt{\varepsilon_{\mathrm{I}}(\mathbf{r}',\omega)}\boldsymbol{G}(\mathbf{r},\mathbf{r}',\omega)\hat{\mathbf{f}}(\mathbf{r}',\omega).\tag{9}$$

Here, $\boldsymbol{G}(\mathbf{r},\mathbf{r}',\omega)$ is the classical Green tensor, which obeys the inhomogeneous, partial differential equation

$$\left[\frac{\omega^2}{c^2}\varepsilon(\mathbf{r},\omega)-\boldsymbol{\nabla}\times\boldsymbol{\nabla}\times\right]\boldsymbol{G}(\mathbf{r},\mathbf{r}',\omega)=-\boldsymbol{\delta}(\mathbf{r}-\mathbf{r}')\tag{10}$$

together with the boundary condition at infinity [$\boldsymbol{\delta}(\mathbf{r})$ is the dyadic δ function], with $\varepsilon(\mathbf{r},\omega)=\varepsilon_{\mathrm{R}}(\mathbf{r},\omega)+i\varepsilon_{\mathrm{I}}(\mathbf{r},\omega)$ being the complex, space- and frequency-dependent permittivity.

Let us consider the case where the particles are constituents of neutral molecules (at positions $\mathbf{r}_M$) that are well separated from each other. The Hamiltonian (1) can then be decomposed into an unperturbed part $\hat{H}_0$ and an interaction part $\hat{H}_{\mathrm{int}}$ as follows:

$$\hat{H}=\hat{H}_0+\hat{H}_{\mathrm{int}},\tag{11}$$

$$\hat{H}_0=\int d^3\mathbf{r}\int_0^\infty d\omega\hbar\omega\,\hat{\mathbf{f}}^\dagger(\mathbf{r},\omega)\hat{\mathbf{f}}(\mathbf{r},\omega)+\sum_M\hat{H}_M,\tag{12}$$

$$\hat{H}_{\mathrm{int}}=\frac{1}{2}\sum_{M\neq M'}\hat{V}_{MM'}+\sum_M\hat{H}_{M\,\mathrm{int}}.\tag{13}$$

Here,

$$\hat{H}_M=\sum_{\alpha_M}\frac{1}{2m_{\alpha_M}}\hat{\mathbf{p}}^2_{\alpha_M}+\frac{1}{2}\hat{V}_{MM}\tag{14}$$

is the Hamiltonian of the Mth molecule,

$$\hat{V}_{MM'}=\sum_{\alpha_M}\sum_{\alpha_{M'}}\frac{q_{\alpha_M}q_{\alpha_{M'}}}{4\pi\varepsilon_0|\hat{\mathbf{r}}_{\alpha_M}-\hat{\mathbf{r}}_{\alpha_{M'}}|}\tag{15}$$

is the Coulomb interaction energy between the Mth and the M'th molecule, and

$$\hat{H}_{M\,\mathrm{int}}=\sum_{\alpha_M}\left(-\frac{q_{\alpha_M}}{m_{\alpha_M}}\right)\hat{\mathbf{p}}_{\alpha_M}\hat{\mathbf{A}}(\hat{\mathbf{r}}_{\alpha_M})+\sum_{\alpha_M}\left(\frac{q_{\alpha_M}^2}{2m_{\alpha_M}}\right)\hat{\mathbf{A}}^2(\hat{\mathbf{r}}_{\alpha_M})+\int d^3\mathbf{r}\,\hat{\rho}_M(\mathbf{r})\hat{\varphi}(\mathbf{r}) \tag{16}$$

is the interaction energy between the Mth molecule [charge density $\hat{\rho}_M(\mathbf{r})$] and the medium-assisted electromagnetic field.

In what follows we shall restrict our attention to the (electric-) dipole approximation, so that Eq. (15) simplifies to

$$\hat{V}_{MM'}=\varepsilon_0^{-1}\mathbf{d}_{M'}\boldsymbol{\delta}^{\parallel}(\mathbf{r}_{M'}-\mathbf{r}_M)\mathbf{d}_M, \tag{17}$$

where

$$\hat{\mathbf{d}}_M=\sum_{\alpha_M}q_{\alpha_M}(\hat{\mathbf{r}}_{\alpha_M}-\mathbf{r}_M) \tag{18}$$

is the dipole operator of the Mth molecule. Disregarding the $\hat{\mathbf{A}}^2$ term in Eq. (16), which does not give rise to off-diagonal molecular matrix elements, making use of Eqs. (6)–(8), and applying the dipole approximation, $\hat{H}_{M\,\mathrm{int}}$ takes the form

$$\hat{H}_{M\,\mathrm{int}}=-\int_0^\infty d\omega\int d^3\mathbf{r}\hat{\boldsymbol{\mu}}_M(\mathbf{r},\omega)\hat{\mathbf{E}}(\mathbf{r},\omega)+\mathrm{H.c.}, \tag{19}$$

where

$$\hat{\boldsymbol{\mu}}_M(\mathbf{r},\omega)=-\frac{1}{\hbar\omega}[\hat{\mathbf{d}}_M,\hat{H}_M]\boldsymbol{\delta}^{\perp}(\mathbf{r}-\mathbf{r}_M)+\hat{\mathbf{d}}_M\boldsymbol{\delta}^{\parallel}(\mathbf{r}-\mathbf{r}_M). \tag{20}$$

B. The transfer rate

Let us consider the resonant energy transfer between two molecules A and B at positions $\mathbf{r}_A$ and $\mathbf{r}_B$. The initial (final) state $|i\rangle$ ($|f\rangle$) describes the excited molecule A (B), the molecule B (A) being in the ground state and the medium-assisted field in the vacuum state,

$$|i\rangle=|a',b\rangle\otimes|\{0\}\rangle,\quad E_i=E_{a'}+E_b, \tag{21}$$

$$|f\rangle=|a,b'\rangle\otimes|\{0\}\rangle,\quad E_f=E_a+E_{b'} \tag{22}$$

(cf. [2]). Note that imposing this initial condition requires that the time of state preparation is sufficiently short compared with the time of energy transfer. Using the Born expansion [19] up to the second order in perturbation theory, the (total) rate of energy transfer can be given by

$$w=\sum_{f,i}p_i w_{fi}, \tag{23}$$

where p_i is the occupation probability of the state $|i\rangle$ and

$$w_{fi}=\frac{2\pi}{\hbar}|\langle f|\hat{T}|i\rangle|^2\delta(E_f-E_i), \tag{24}$$

with

$$\hat{T}=\hat{H}_{\mathrm{int}}+\hat{H}_{\mathrm{int}}\frac{1}{E_i-\hat{H}_0+is}\hat{H}_{\mathrm{int}},\quad s\to+0. \tag{25}$$

Applying the decomposition (13), we may write

$$\langle f|\hat{T}|i\rangle=\langle a,b'|\hat{T}|a',b\rangle=\langle a,b'|\hat{V}_{AB}|a',b\rangle+\langle a,b'|\hat{\mathcal{T}}|a',b\rangle, \tag{26}$$

where

$$\langle a,b'|\hat{\mathcal{T}}|a',b\rangle=\langle a,b'|[\hat{H}_{A\,\mathrm{int}}+\hat{H}_{B\,\mathrm{int}}][E_i-\hat{H}_0+is]^{-1}\times[\hat{H}_{A\,\mathrm{int}}+\hat{H}_{B\,\mathrm{int}}]|a',b\rangle. \tag{27}$$

Let us first consider the Coulomb term $\langle a,b'|\hat{V}_{AB}|a',b\rangle$. From Eq. (17) it is not difficult to see that

$$\langle a,b'|\hat{V}_{AB}|a',b\rangle=\varepsilon_0^{-1}[\mathbf{d}_{b'b}\boldsymbol{\delta}^{\parallel}(\mathbf{r}_B-\mathbf{r}_A)\mathbf{d}_{aa'}], \tag{28}$$

where

$$\mathbf{d}_{aa'(bb')}=\langle a(b)|\hat{\mathbf{d}}_{A(B)}|a'(b')\rangle. \tag{29}$$

In order to calculate $\langle a,b'|\hat{\mathcal{T}}|a',b\rangle$, we make use of Eqs. (19) and (20), perform the summation and integrations over the possible intermediate states $|a',b'\rangle\hat{f}_j^{\dagger}(\mathbf{s},\omega)|\{0\}\rangle$ and $|a,b\rangle\hat{f}_j^{\dagger}(\mathbf{s},\omega)|\{0\}\rangle$. After some calculation we derive, on applying Eq. (9) and the relationship [16,17]

$$\mathrm{Im}\,G_{kl}(\mathbf{r},\mathbf{r}',\omega)=\int d^3\mathbf{s}\frac{\omega^2}{c^2}\varepsilon_1(\mathbf{s},\omega)G_{km}(\mathbf{r},\mathbf{s},\omega)G_{lm}^*(\mathbf{r}',\mathbf{s},\omega), \tag{30}$$

the following expression:

$$\langle a,b'|\hat{\mathcal{T}}|a',b\rangle=\frac{\hbar\omega_{a'a}^2}{\pi\varepsilon_0c^2}\int d^3\mathbf{r}'\int d^3\mathbf{r}\int_0^\infty d\omega\left\{\frac{[\mathbf{d}_{b'b}\boldsymbol{\Delta}_B(\mathbf{r}',-\omega)\mathrm{Im}\,\boldsymbol{G}(\mathbf{r}',\mathbf{r},\omega)\boldsymbol{\Delta}_A(\mathbf{r},-\omega)\mathbf{d}_{aa'}]}{-\hbar\omega_{a'a}-\hbar\omega+is}+\frac{[\mathbf{d}_{b'b}\boldsymbol{\Delta}_B(\mathbf{r}',\omega)\mathrm{Im}\,\boldsymbol{G}(\mathbf{r}',\mathbf{r},\omega)\boldsymbol{\Delta}_A(\mathbf{r},\omega)\mathbf{d}_{aa'}]}{\hbar\omega_{a'a}-\hbar\omega+is}\right\}, \tag{31}$$

where

$$\omega_{a'a}=(E_{a'}-E_a)/\hbar=(E_{b'}-E_b)/\hbar=\omega_{b'b} \tag{32}$$

and

$$\boldsymbol{\Delta}_{A(B)}(\mathbf{r},\omega)=\boldsymbol{\delta}^{\perp}(\mathbf{r}-\mathbf{r}_{A(B)})+\frac{\omega}{\omega_{a'a(b'b)}}\boldsymbol{\delta}^{\parallel}(\mathbf{r}-\mathbf{r}_{A(B)}) \tag{33}$$

[note that $\boldsymbol{\Delta}_{A(B)}(\mathbf{r},\omega_{a'a(b'b)})=\boldsymbol{\delta}(\mathbf{r}-\mathbf{r}_{A(B)})$]. Recalling that $\mathrm{Im}\,\boldsymbol{G}(\mathbf{r}',\mathbf{r},-\omega)=-\mathrm{Im}\,\boldsymbol{G}(\mathbf{r}',\mathbf{r},\omega)$, we may rewrite Eq. (31) as

$$\langle a,b'|\hat{T}|a',b\rangle=\frac{\hbar\omega_{a'a}^2}{\pi\varepsilon_0 c^2}\int d^3\mathbf{r}'\int d^3\mathbf{r}\int_{-\infty}^{\infty}d\omega\,\frac{1}{2i}\left\{\left[\frac{[\mathbf{d}_{b'b}\boldsymbol{\Delta}_B(\mathbf{r}',\omega)\boldsymbol{G}(\mathbf{r}',\mathbf{r},\omega)\boldsymbol{\Delta}_A(\mathbf{r},\omega)\mathbf{d}_{aa'}]}{\hbar\omega_{a'a}-\hbar\omega+is\,\mathrm{sgn}(\omega)}\right]\right.$$
$$\left.-\left[\frac{[\mathbf{d}_{bb'}\boldsymbol{\Delta}_B(\mathbf{r}',\omega)\boldsymbol{G}(\mathbf{r}',\mathbf{r},\omega)\boldsymbol{\Delta}_A(\mathbf{r},\omega)\mathbf{d}_{a'a}]}{\hbar\omega_{a'a}-\hbar\omega-is\,\mathrm{sgn}(\omega)}\right]^*\right\}. \tag{35}$$

The ω integral in Eq. (35) may now be evaluated by means of contour-integral techniques, by taking into account the fact that the Green tensor is a holomorphic function of ω in the upper complex half plane, which asymptotically behaves as [17]

$$\lim_{|\omega|\to\infty}\frac{\omega^2}{c^2}\boldsymbol{G}(\mathbf{r},\mathbf{r}',\omega)=-\boldsymbol{\delta}(\mathbf{r}-\mathbf{r}'). \tag{36}$$

We therefore close the path of integration by an infinitely large semicircle in the upper complex half plane, $|\omega|\to\infty$, and subsequently subtract the semicircle integral. It is easily seen that only the terms in $\boldsymbol{\Delta}_A(\mathbf{r},\omega)$ and $\boldsymbol{\Delta}_B(\mathbf{r},\omega)$ [Eq. (33)], which are proportional to ω, contribute to the integral over the semicircle,

$$\langle a,b'|\hat{T}|a',b\rangle|_{\text{semicircle}}=\varepsilon_0^{-1}[\mathbf{d}_{b'b}\boldsymbol{\delta}^{\parallel}(\mathbf{r}_B-\mathbf{r}_A)\mathbf{d}_{aa'}]. \tag{37}$$

It is further seen that only the first term in the curly bracket contributes to the integral over the closed path. We thus arrive at

$$\langle a,b'|\hat{T}|a',b\rangle=-\varepsilon_0^{-1}[\mathbf{d}_{b'b}\boldsymbol{\delta}^{\parallel}(\mathbf{r}_B-\mathbf{r}_A)\mathbf{d}_{aa'}]$$
$$-\frac{\omega_{a'a}^2}{\varepsilon_0 c^2}[\mathbf{d}_{b'b}\boldsymbol{G}(\mathbf{r}_B,\mathbf{r}_A,\omega_{a'a})\mathbf{d}_{aa'}]. \tag{38}$$

Substitution of the expressions (28) and (38) into Eq. (26) yields the transition amplitude

$$\langle a,b'|\hat{T}|a',b\rangle=\frac{\hbar\omega_{a'a}^2}{\pi\varepsilon_0 c^2}\int d^3\mathbf{r}'\int d^3\mathbf{r}\int_{-\infty}^{\infty}d\omega\,\frac{[\mathbf{d}_{b'b}\boldsymbol{\Delta}_B(\mathbf{r}',\omega)\mathrm{Im}\,\boldsymbol{G}(\mathbf{r}',\mathbf{r},\omega)\boldsymbol{\Delta}_A(\mathbf{r},\omega)\mathbf{d}_{aa'}]}{\hbar\omega_{a'a}-\hbar\omega+is\,\mathrm{sgn}(\omega)} \tag{34}$$

or, equivalently,

$$\langle a,b'|\hat{T}|a',b\rangle=-\frac{\omega_{a'a}^2}{\varepsilon_0 c^2}[\mathbf{d}_{b'b}\boldsymbol{G}(\mathbf{r}_B,\mathbf{r}_A,\omega_{a'a})\mathbf{d}_{aa'}]. \tag{39}$$

Note that the first term in Eq. (38) and the Coulomb term (28) exactly cancel out. We eventually combine Eqs. (24) and (39) and find that the rate of energy transfer between the chosen states $|a',b\rangle$ and $|a,b'\rangle$ reads as ($w_{fi}=w_{ab'}^{a'b}$)

$$w_{ab'}^{a'b}=\frac{2\pi}{\hbar^2}\left(\frac{\omega_{a'a}^2}{\varepsilon_0 c^2}\right)^2|\mathbf{d}_{b'b}\boldsymbol{G}(\mathbf{r}_B,\mathbf{r}_A,\omega_{a'a})\mathbf{d}_{aa'}|^2$$
$$\times\delta(\omega_{a'a}-\omega_{b'b}). \tag{40}$$

It can be proved (Appendix A) that the use of the multipolar Hamiltonian [17] instead of the minimal-coupling Hamiltonian (1) exactly leads to the same expression of the energy-transfer rate.

Let us now consider the total energy-transfer rate according to Eq. (23), by taking into account the vibronic structure of the molecular energy levels. Restricting our attention to the Born-Oppenheimer approximation and neglecting the weak dependence of the electronic-dipole-transition matrix element on the nuclear coordinates (see, e.g., [20]), we may factorize the dipole-transition matrix elements according to

$$\mathbf{d}_{aa'(bb')}=\mathbf{d}_{A(B)}v_{aa'(bb')}, \tag{41}$$

where $\mathbf{d}_A(\mathbf{d}_B)$ is the purely electronic transition-dipole matrix element of the transition between the lower and the upper electronic state of the molecule A (B), and $v_{aa'(bb')}$ are the overlap integrals between the vibrational quantum states in the two electronic states of the respective molecule. Note

that the vibrational overlap integrals take account of both displaced and distorted energy surfaces. Combining Eqs. (23) and (40) yields

$$w=\frac{2\pi}{\hbar^2}\sum_{a,a'}\sum_{b,b'}p_{a'}p_b\left(\frac{\omega_{a'a}^2}{\varepsilon_0 c^2}\right)^2|v_{b'b}v_{aa'}|^2 \times|\mathbf{d}_B^*\boldsymbol{G}(\mathbf{r}_B,\mathbf{r}_A,\omega_{a'a})\mathbf{d}_A|^2\delta(\omega_{a'a}-\omega_{b'b}), \quad (42)$$

which can be rewritten as

$$w=\int d\omega\tilde{w}(\omega)\sigma_A^{\mathrm{em}}(\omega)\sigma_B^{\mathrm{abs}}(\omega), \quad (43)$$

where

$$\tilde{w}(\omega)=\frac{2\pi}{\hbar^2}\left(\frac{\omega^2}{\varepsilon_0 c^2}\right)^2|\mathbf{d}_B^*\boldsymbol{G}(\mathbf{r}_B,\mathbf{r}_A,\omega)\mathbf{d}_A|^2, \quad (44)$$

and

$$\sigma_A^{\mathrm{em}}(\omega)=\sum_{a,a'}p_{a'}|v_{aa'}|^2\delta(\omega_{a'a}-\omega) \quad (45)$$

and

$$\sigma_B^{\mathrm{abs}}(\omega)=\sum_{b,b'}p_b|v_{b'b}|^2\delta(\omega_{b'b}-\omega), \quad (46)$$

respectively, are proportional to the (single-photon) emission spectrum of molecule *A* and the (single-photon) absorption spectrum of molecule *B*, both in *free space* [20]. Thus, the rate of energy transfer is proportional to the overlap of the two spectra weighted by the square of the absolute value of the actual Green tensor. It is worth mentioning that Eqs. (40)–(46) apply to the resonant energy transfer between two molecules in the presence of an arbitrary configuration of dispersing and absorbing macroscopic bodies. All the relevant parameters of the bodies are contained in the Green tensor. Note that the emission (absorption) spectrum observed in this case is not proportional to $\sigma_A^{\mathrm{em}}(\omega)[\sigma_B^{\mathrm{abs}}(\omega)]$, in general, as it can be seen from a comparison of Eq. (45) with Eq. (B7).

In particular when the Green tensor slowly varies with frequency on a scale given by the (relevant) vibrational frequencies of the molecules, then $\tilde{w}(\omega)$ is also a slowly varying function of frequency and can (approximately) be taken at the electronic-energy-transfer frequency $\omega_A(\approx\omega_B)$ and put in front of the integral in Eq. (43); thus

$$w\simeq\tilde{w}(\omega_A)\sigma, \quad (47)$$

where

$$\sigma=\int d\omega\sigma_A^{\mathrm{em}}(\omega)\sigma_B^{\mathrm{abs}}(\omega). \quad (48)$$

In this case, the influence of matter environment on the (total) energy-transfer rate is fully contained in $\tilde{w}(\omega_A)$. Clearly, when the two molecules are near a resonatorlike equipment, so that the molecule can ''feel'' sharply peaked field resonances, then $\tilde{w}(\omega)$ cannot be assumed to be a slowly varying function of frequency, in general (see Sec. III C).

It may be interesting to compare the rate of energy transfer with the donor decay rate. Straightforward generalization of the well-known formula for a two-level transition yields, on applying the Born-Oppenheimer approximation,

$$\Gamma_A=\int d\omega\tilde{\Gamma}_A(\omega)\sigma_A^{\mathrm{em}}(\omega), \quad (49)$$

where

$$\tilde{\Gamma}_A(\omega)=\frac{2\omega^2}{\hbar\varepsilon_0 c^2}[\mathbf{d}_A^*\mathrm{Im}\,\boldsymbol{G}(\mathbf{r}_A,\mathbf{r}_A,\omega)\mathbf{d}_A] \quad (50)$$

and $\sigma_A^{\mathrm{em}}(\omega)$ is given by Eq. (45). Whereas the decay rate is determined by the imaginary part of the Green tensor (taken at equal positions), the transfer rate is determined by the full Green tensor (taken at different positions). Thus, decay rate and transfer rate can quite differently respond to a change of the environment.

III. APPLICATIONS

A. Bulk material

Let us first consider the case when the two molecules are embedded in bulk material of arbitrary complex permittivity $\varepsilon(\omega)$. Using the well-known expression of the bulk-material Green tensor $\boldsymbol{G}^{\mathrm{bulk}}(\mathbf{r},\mathbf{r}',\omega)$ (see, e.g., [17]), application of Eq. (44) yields

$$\tilde{w}(\omega)=\frac{2\pi}{\hbar^2}\left(\frac{\omega^2}{\varepsilon_0 c^2}\right)^2|\mathbf{d}_B^*\boldsymbol{G}^{\mathrm{bulk}}(\mathbf{r}_B,\mathbf{r}_A,\omega)\mathbf{d}_A|^2, \quad (51)$$

where

$$\mathbf{d}_B^*\boldsymbol{G}^{\mathrm{bulk}}(\mathbf{r}_B,\mathbf{r}_A,\omega)\mathbf{d}_A=\frac{q(\omega)}{4\pi}\exp[iq(\omega)R] \times\left[-\left(\mathbf{d}_B^*\mathbf{d}_A-3\frac{\mathbf{d}_B^*\mathbf{R}}{R}\frac{\mathbf{d}_A\mathbf{R}}{R}\right)\times\left(\frac{1}{q^3(\omega)R^3}-\frac{i}{q^2(\omega)R^2}\right)+\left(\mathbf{d}_B^*\mathbf{d}_A-\frac{\mathbf{d}_B^*\mathbf{R}}{R}\frac{\mathbf{d}_A\mathbf{R}}{R}\right)\frac{1}{q(\omega)R}\right] \quad (52)$$

with

$$q(\omega)=\sqrt{\varepsilon(\omega)}\,\frac{\omega}{c},\quad \mathbf{R}=\mathbf{r}_B-\mathbf{r}_A. \quad (53)$$

The energy-transfer rate is then obtained according to Eq. (43). Obviously, the Green tensor of bulk material can be

regarded as being a slowly varying function of frequency, so that approximation (47) applies.

From Eqs. (51) and (52) it is seen that the energy-transfer rate includes both the small-distance case (Förster transfer), with the rate being proportional to R^{-6}, and the large-distance (radiative) case, where the rate becomes proportional to R^{-2}. Note that the exponential $|\exp[iq(\omega)R]|^2 = \exp[-2\omega n_I(\omega)R/c]$, which typically arises from material absorption, drastically diminishes the large-distance energy transfer $[\sqrt{\varepsilon(\omega)} = n(\omega) = n_R(\omega) + in_I(\omega)]$. In Eq. (51) local-field corrections are ignored. They may be taken into account by applying, e.g., the scheme used in Ref. [18] for correcting the rate of spontaneous decay.

It is worth noting that the result given above, which is based on the quantization of the macroscopic Maxwell field for given complex permittivity, exactly corresponds to the result obtained in Ref. [9] within the framework of a fully microscopic approach on the basis of some model medium coupled to the radiation field and a heat bath. Already from the study of the spontaneous decay of an excited atom near an interface [21] it is clear that in the case of inhomogeneous media (of complicated atomic structure) a microscopic approach would be rather involved and closed solutions would hardly be found.

B. Multislab planar structures

Let us consider a planar multislab structure and assume that the two molecules are in the same slab. The relevant Green tensor (for the energy transfer between the two molecules) of an inhomogeneous system of this type can always be written in the form

$$\boldsymbol{G}(\mathbf{r}_B,\mathbf{r}_A,\omega) = \boldsymbol{G}^{\mathrm{bulk}}(\mathbf{r}_B,\mathbf{r}_A,\omega) + \boldsymbol{G}^{\mathrm{refl}}(\mathbf{r}_B,\mathbf{r}_A,\omega), \quad (54)$$

where $\boldsymbol{G}^{\mathrm{bulk}}(\mathbf{r}_B,\mathbf{r}_A,\omega)$ is the Green tensor according to Eq. (52), with $\varepsilon(\omega)$ being the permittivity of the slab in which the two molecules are located, and the reflection term $\boldsymbol{G}^{\mathrm{refl}}(\mathbf{r}_B,\mathbf{r}_A,\omega)$ ensures the correct boundary conditions at the surfaces of discontinuity. Clearly, a decomposition of the type of Eq. (54) is also valid for other than planar systems, provided that the two molecules are located in a region of space-independent permittivity.

To be more specific, let the z direction be the direction of variation of the permittivity of the multislab system and assume that $\mathbf{r}_A$ and $\mathbf{r}_B$ are in the jth slab of thickness d_j (Fig. 1). The reflection term in Eq. (54) can then be given by [22] (see also Ref. [23])

$$\boldsymbol{G}^{\mathrm{refl}}(\mathbf{r}_B,\mathbf{r}_A,\omega) = \frac{i}{4\pi}\int_0^\infty \frac{dk_\parallel k_\parallel}{2\beta_j} e^{i\beta_j d_j}\tilde{\boldsymbol{G}}^{\mathrm{refl}}(\mathbf{r}_B,\mathbf{r}_A,\omega,k_\parallel) \quad (55)$$

$[k_j = \sqrt{\varepsilon_j(\omega)}\omega/c, \beta_j = (k_j^2 - k_\parallel^2)^{1/2}]$. Choosing the coordinate system such that $R_y = 0$, the nonvanishing components of $\tilde{\boldsymbol{G}}^{\mathrm{refl}}$ read

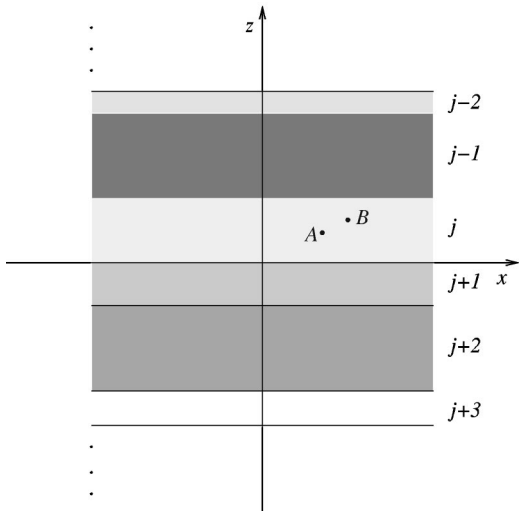

FIG. 1. Geometry of the multislab planar structure problem.

$$\tilde{G}^{\mathrm{refl}}_{xx(yy)} = -\frac{\beta_j^2}{k_j^2} C_-^p [J_0(k_\parallel R_x) - (+) J_2(k_\parallel R_x)] + C_+^s [J_0(k_\parallel R_x) + (-) J_2(k_\parallel R_x)], \quad (56)$$

$$\tilde{G}^{\mathrm{refl}}_{xz(zx)} = -(+) 2i \frac{\beta_j k_\parallel}{k_j^2} S^p_{+(-)} J_1(k_\parallel R_x), \quad (57)$$

$$\tilde{G}^{\mathrm{refl}}_{zz} = 2\frac{k_\parallel^2}{k_j^2} C_+^p J_0(k_\parallel R_x) \quad (58)$$

[$J_n(x)$ is a Bessel function], where

$$C^q_{+(-)} = [r^q_- e^{i\beta_j(z_A+z_B-d_j)} + r^q_+ e^{-i\beta_j(z_A+z_B-d_j)} + (-) 2 r^q_+ r^q_- \cos(\beta_j R_z) e^{i\beta_j d_j}] D_q^{-1}, \quad (59)$$

$$S^q_{+(-)} = [r^q_- e^{i\beta_j(z_A+z_B-d_j)} - r^q_+ e^{-i\beta_j(z_A+z_B-d_j)} + (-) 2 i r^q_+ r^q_- \sin(\beta_j R_z) e^{i\beta_j d_j}] D_q^{-1}, \quad (60)$$

$$D_q = 1 - r^q_+ r^q_- e^{2i\beta_j d_j}. \quad (61)$$

Here, $q = p$ (s) means TM (TE) polarized waves and $r^q_{+(-)}$ are the total reflection coefficients at the upper (lower) stack of slabs $[j' < j (j' > j)]$ of the waves in the jth slab (for details, see Ref. [22]). Note that when $\mathbf{r}_A$ and $\mathbf{r}_B$ are in the top (bottom) slab, then Eqs. (55)–(61) (formally) apply provided that $r^q_{+(-)} = 0$ and $d_j = 0$ are set.

If the frequencies of the vibronic transitions that are involved in the energy transfer are sufficiently far from a medium resonance, so that material absorption (in the jth slab) may be disregarded, then the permittivity may be considered as being real and positive. In this case, it may be useful to decompose the integral in Eq. (55) into two parts,

$$\boldsymbol{G}^{\mathrm{refl}}(\mathbf{r}_B,\mathbf{r}_A,\omega) = \boldsymbol{G}_1^{\mathrm{refl}}(\mathbf{r}_B,\mathbf{r}_A,\omega) + \boldsymbol{G}_2^{\mathrm{refl}}(\mathbf{r}_B,\mathbf{r}_A,\omega), \quad (62)$$

$$\boldsymbol{G}_1^{\mathrm{refl}}(\mathbf{r}_B,\mathbf{r}_A,\omega)=\frac{i}{4\pi}\int_0^{\sqrt{\varepsilon_j}\omega/c}\frac{dk_\parallel k_\parallel}{2\beta_j}e^{i|\beta_j|d_j}\tilde{\boldsymbol{G}}^{\mathrm{refl}}\times(\mathbf{r}_B,\mathbf{r}_A,\omega,k_\parallel), \tag{63}$$

$$\boldsymbol{G}_2^{\mathrm{refl}}(\mathbf{r}_B,\mathbf{r}_A,\omega)=\frac{i}{4\pi}\int_{\sqrt{\varepsilon_j}\omega/c}^{\infty}\frac{dk_\parallel k_\parallel}{2\beta_j}e^{-|\beta_j|d_j}\tilde{\boldsymbol{G}}^{\mathrm{refl}}(\mathbf{r}_B,\mathbf{r}_A,\omega,k_\parallel). \tag{64}$$

Obviously, $\boldsymbol{G}_1^{\mathrm{refl}}$ results from waves that have a propagating component in the z direction, whereas the waves that contribute to $\boldsymbol{G}_2^{\mathrm{refl}}$ are purely evanescent in the z direction.

1. Interface

Let the two molecules be embedded in a half-space medium (medium 1) and assume that in the relevant frequency interval the permittivity of the medium $\varepsilon_1(\omega)$ can be regarded as being real and positive. When the molecules are near the interface between the two half-space media such that $k_1(z_A+z_B)\ll 1$, it can be proved that Eqs. (55)–(58) reduce to $(k_1R_x\ll 1)$

$$G_{xx(yy)}^{\mathrm{refl}}(\mathbf{r}_B,\mathbf{r}_A,\omega)\simeq\frac{1}{4\pi k_1^2}\frac{\varepsilon_2-\varepsilon_1}{\varepsilon_2+\varepsilon_1}\frac{(z_A+z_B)^2-(+)2R_x^2}{[(z_A+z_B)^2+R_x^2]^{5/2}}, \tag{65}$$

$$G_{xz(zx)}^{\mathrm{refl}}(\mathbf{r}_B,\mathbf{r}_A,\omega)\simeq+(-)\frac{1}{4\pi k_1^2}\frac{\varepsilon_2-\varepsilon_1}{\varepsilon_2+\varepsilon_1}\times\frac{3(z_A+z_B)R_x}{[(z_A+z_B)^2+R_x^2]^{5/2}}, \tag{66}$$

$$G_{zz}^{\mathrm{refl}}(\mathbf{r}_B,\mathbf{r}_A,\omega)\simeq\frac{1}{4\pi}\frac{\varepsilon_2-\varepsilon_1}{\varepsilon_2+\varepsilon_1}\frac{1}{\sqrt{(z_A+z_B)^2+R_x^2}}\times\left\{\frac{2(z_A+z_B)^2-R_x^2}{k_1^2[(z_A+z_B)^2+R_x^2]^2}+1\right\} \tag{67}$$

[$\varepsilon_2(\omega)$ is the complex permittivity of medium 2]. Note that for $\mathbf{r}_A=\mathbf{r}_B$, Eqs. (65)–(67) just give the Green tensor whose imaginary part determines the influence of the interface on the rate of spontaneous decay of a single molecule [21,24]. (For some special cases, see also Ref. [15].) Under the assumptions made, the main contribution to $\boldsymbol{G}^{\mathrm{refl}}$ comes from $\boldsymbol{G}_2^{\mathrm{refl}}$. Hence surface-guided waves (including decaying waves) play an important role and can noticeably influence the resonant energy transfer. In particular, when medium 2 is a metal or a dielectric with $\varepsilon_{2\,\mathrm{R}}<0$ (and typically $\varepsilon_{2\,\mathrm{I}}\ll|\varepsilon_{2\,\mathrm{R}}|$), then a strong effect is observed for $\varepsilon_{2\,\mathrm{R}}(\omega)=-\varepsilon_1(\omega)$, which is nothing but the condition for best excitation of surface-guided waves [25].

In the numerical calculation of $\tilde{w}(\omega)$ [Eq. (44)], which contains the relevant information about the influence of the interface on the rate of energy transfer [see Eqs. (43)–(46)], we have assumed that the two molecules are situated in vacuum [$\varepsilon_1(\omega)=1$] above a half-space medium of the Drude-Lorentz type and have restricted our attention to a single-resonance medium,

$$\varepsilon_2(\omega)\equiv\varepsilon(\omega)=1+\frac{\omega_{\mathrm{P}}^2}{\omega_{\mathrm{T}}^2-\omega^2-i\omega\gamma}. \tag{68}$$

Here, ω_{P} corresponds to the coupling constant and ω_{T} and γ are, respectively, the medium-oscillation frequency and the linewidth. Recall that the Drude-Lorentz model covers both metallic ($\omega_{\mathrm{T}}=0$) and dielectric ($\omega_{\mathrm{T}}\neq 0$) matter and features a band gap between ω_{T} and $\omega_{\mathrm{L}}=\sqrt{\omega_{\mathrm{T}}^2+\omega_{\mathrm{P}}^2}$. We have performed the calculations using the exact Green tensor [Eqs. (54)–(61)]. Comparing the results with those obtained by using the approximately valid Green tensor [Eq. (54) together with Eqs. (65)–(67)], we have found good agreement.

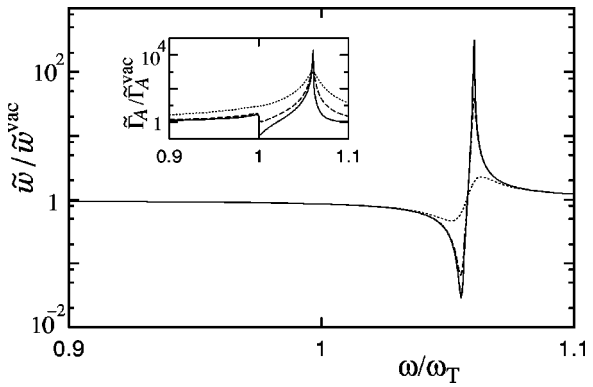

FIG. 2. The electronic part of the rate of energy transfer [Eq. (44)] between two molecules near a planar dielectric half space is shown as a function of the transition frequency for z-oriented dipole-transition moments and a single-resonance Drude-Lorentz-type dielectric [$R_x=0.015\lambda_{\mathrm{T}}$, $z_A=z_B=0.02\lambda_{\mathrm{T}}$, $\omega_{\mathrm{P}}=0.5\omega_{\mathrm{T}}$, $\gamma/\omega_{\mathrm{T}}=10^{-4}$ (solid line), 10^{-3} (dashed line), and 10^{-2} (dotted line)]. The inset shows the electronic part of the corresponding donor-decay rate [Eq. (50)].

The behavior of $\tilde{w}(\omega)$ is illustrated in Fig. 2. It is seen that outside the band gap ($\omega<\omega_{\mathrm{T}}$), where $\varepsilon_{\mathrm{R}}>0$, the modification of $\tilde{w}(\omega)$ due to the presence of the interface is small even for small distances of the molecules from the interface. Since in this frequency domain $\tilde{w}(\omega)$ may be regarded as being slowly varying on a frequency scale defined by the vibrational frequencies of the molecules, Eq. (47) applies. Thus, the energy-transfer rate is simply proportional to $\tilde{w}(\omega_A)$.

Inside the band gap, however, the interface can significantly affect $\tilde{w}(\omega)$ if, according to Eqs. (65)–(67), $\varepsilon_{\mathrm{R}}(\omega)\simeq-1$ ($\omega\simeq 1.06\,\omega_{\mathrm{T}}$ in Fig. 2), that is to say, if the energy-transfer transition under consideration is tuned to a surface-guided wave. Note that a negative real part of the medium permittivity can easily be realized by metals. Careful inspection of the contributions $\boldsymbol{G}^{\mathrm{vac}}$ and $\boldsymbol{G}^{\mathrm{refl}}$ to $\boldsymbol{G}$ reveals that the enhancement of $\tilde{w}(\omega)$ results from $\boldsymbol{G}^{\mathrm{refl}}$, whereas the reduction reflects some destructive interference of $\boldsymbol{G}^{\mathrm{vac}}$ and $\boldsymbol{G}^{\mathrm{refl}}$. Another interesting feature is that the reduction of $\tilde{w}(\omega)$ can

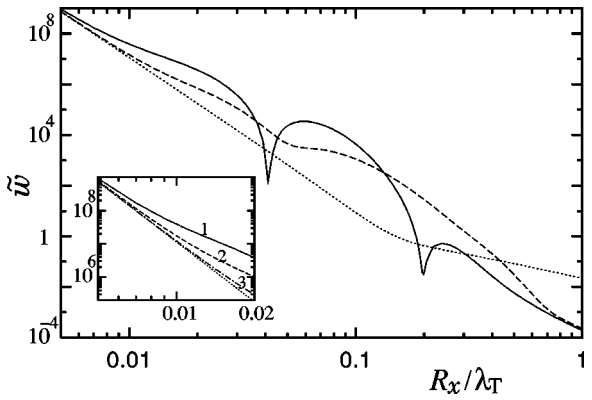

FIG. 3. The electronic part of the rate of energy transfer (Eq. (44), in units of $[|d_A d_B|\omega^3/(\hbar\varepsilon_0 c^3)]^2/(8\pi)$) between two molecules near a planar dielectric half space is shown as a function of the intermolecular distance for z-oriented dipole-transition moments and a single-resonance Drude-Lorentz-type dielectric [$\omega=1.062\omega_T$, $z_A=z_B=0.02\lambda_T$, $\omega_P=0.5\omega_T$, $\gamma/\omega_T=10^{-4}$ (solid line) and 10^{-2} (dashed line)]. The dependence of $\tilde{w}$ on the molecule-interface distance is illustrated in the inset [$\gamma/\omega_T=10^{-4}$, $z_A=z_B=0.02\lambda_T$ (curve 1), $0.03\lambda_T$ (curve 2), and $0.05\lambda_T$ (curve 3)]. For comparison, the free-space result is shown (dotted lines).

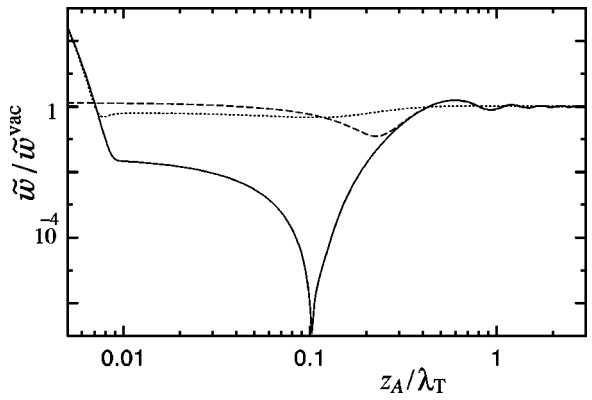

FIG. 4. The electronic part of the rate of energy transfer [Eq. (44)] between two molecules near a planar dielectric half space is shown as a function of the distance of the molecules from the surface ($z_A=z_B$) for z-oriented dipole-transition moments and a single-resonance Drude-Lorentz-type dielectric ($R_x=0.85\lambda_T$; $\omega_P=0.5\,\omega_T$; $\gamma/\omega_T=10^{-4}$). For comparison, the results that are obtained by taking into account in Eq. (62) only $\boldsymbol{G}_1^{\mathrm{refl}}$ (dashed line) or $\boldsymbol{G}_2^{\mathrm{refl}}$ (dotted line) are shown.

go hand in hand with an enhancement of the corresponding quantity $\tilde{\Gamma}_A(\omega)$ [Eq. (50)] for the donor-decay rate Γ_A [Eq. (49)] (see the inset in Fig. 2).

Further, Fig. 2 reveals that with increasing material absorption (i.e., with increasing value of γ) $\tilde{w}(\omega)$ varies less rapidly inside the band-gap region, and enhancement and reduction are thus less pronounced. Clearly, the strong influence on $\tilde{w}(\omega)$ of the interface, which is observed for small material absorption, must not necessarily lead to a corresponding strong change of the energy-transfer rate, because of the integration in Eq. (43). Nevertheless, the results show the possibility of controlling the resonant energy transfer by surface-guided waves.

Figure 3 illustrates the dependence of $\tilde{w}(\omega)$ on the intermolecular distance for the case when ω corresponds to a surface-guided wave frequency and a noticeable change of $\tilde{w}(\omega)$ is observed ($\omega=1.062\,\omega_T$ in the figure). It is seen that the R_x^{-6} dependence, which is typical of the Förster transfer in free space, is observed for much shorter intermolecular distances. The relative minima of $\tilde{w}(\omega)$ below the free-space level, which are observed for somewhat larger intermolecular distances, again result from destructive interference between $\boldsymbol{G}^{\mathrm{vac}}$ and $\boldsymbol{G}^{\mathrm{refl}}$. Eventually, the large-distance reduction of $\tilde{w}(\omega)$ below the free-space level results from material absorption. As already mentioned, the behavior of $\tilde{w}(\omega)$ in Fig. 3 is dominated by surface-guided waves that decay exponentially along the $\pm z$ directions. With increasing material absorption the penetration depths decrease, so that on average $\tilde{w}(\omega)$ becomes closer to the free-space level. The possibility of controlling the ultrashort-range energy transfer by varying the distance of the molecule from the surface is illustrated in the inset.

In Fig. 4 the dependence of $\tilde{w}(\omega)$ (again for $\omega\simeq1.062\,\omega_T$) on the molecule-surface distance is plotted, and the contributions to $\tilde{w}(\omega)$ from ordinary waves having a propagating component in the z direction ($\boldsymbol{G}_1^{\mathrm{refl}}$) and surface-guided waves ($\boldsymbol{G}_2^{\mathrm{refl}}$) are shown. It is clearly seen that when the two molecules are very near the surface, then energy transfer between them is mediated by surface-guided waves, whereas for larger distances ordinary waves play the dominant role. Note that the oscillatory behavior is typical of the latter case. Clearly, for very large distances ($z_A, z_B \gg \lambda_T$) the free-space behavior is observed.

2. Comparison with experiments

Recently, experiments have been carried out to study the transfer of excitation energy between dye molecules confined within planar optical microcavities [8]. In the experiments, donors (Eu^{3+} complex) and acceptors (1,1′-dioctadecyl-3,3,3′,3′-tetramethylindodicarbocyanine) embedded within a transparent material (22-tricosenoic acid) bounded by no (weak-cavity structure) mirror, one (half-cavity structure) silver mirror, or two (full-cavity structure) silver mirrors are considered. To compare the experimental results with the theoretical ones, we have modeled the half-cavity structure by a planar four-layered system and the full-cavity structure by a five-layered system. The former consists of vacuum, dielectric matter (22-tricosenoic acid, $\varepsilon=2.49$ [26], thickness d), metal (silver, $\varepsilon=-16.0+0.6i$ [26], thickness 25 nm), and vacuum, and the latter consists of vacuum, metal (silver, thickness 20 nm), dielectric matter (the same as above, thickness d), metal (silver, thickness 25 nm), and vacuum. In each system, the donor is situated in the middle of the dielectric layer, while the position of the acceptor is shifted towards the silver mirror of 25 nm thickness. The Green tensors of the two systems can be calculated according to Eqs. (54)–(61). Assigning to silver a Drude-Lorentz-type permittivity [27], it can be proven that in the relevant frequency interval (of overlapping donor emission

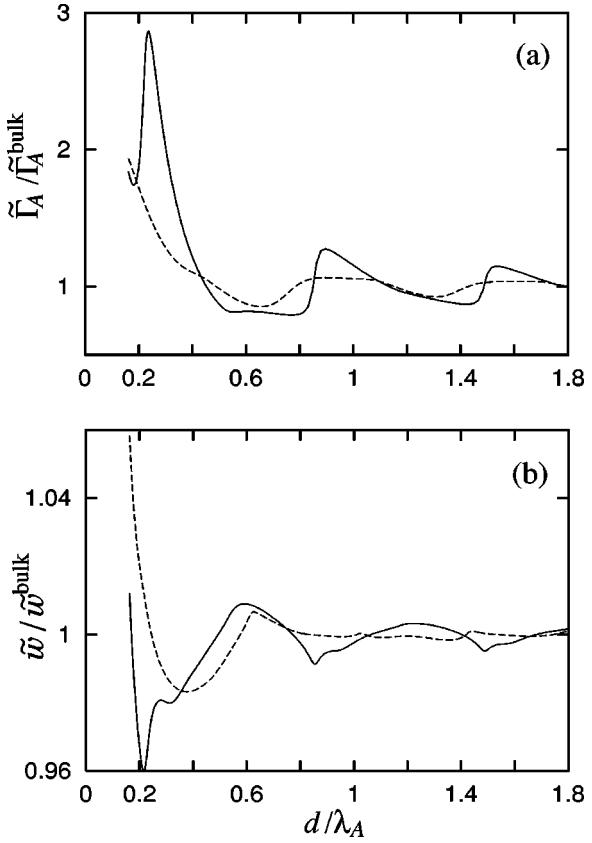

FIG. 5. The electronic parts of the donor-decay rate (a) and the donor-acceptor energy-transfer rate (b) (averaged over the dipole orientations) of molecules in cavitylike systems are shown as functions of the cavity length for the four-layered system (dashed line) and the five-layered system (full line) considered in Sec. III B 2 ($\lambda_A = 614$ nm; $R = -R_z = 24$ nm).

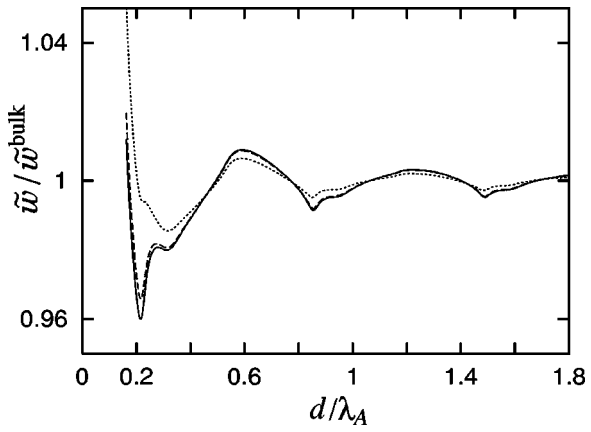

FIG. 6. The electronic part of the donor-acceptor energy-transfer rate (averaged over the dipole orientations) of molecules in the five-layered cavitylike system considered in Sec. III B 2 is shown as a function of the cavity length for various values of the intermolecular distance [$\lambda_A = 614$ nm, $R_z = -24$ nm, $R_x = 0$ (solid line), 10 nm (dashed line), and 20 nm (dotted line)].

and acceptor absorption spectra) $\tilde{w}(\omega)$ [Eq. (44)] and $\tilde{\Gamma}_A(\omega)$ [Eq. (50)] vary sufficiently slowly with ω, so that [cf. Eq. (47)] $w \sim \tilde{w}(\omega_A)$ and, similarly, $\Gamma_A \sim \tilde{\Gamma}_A(\omega_A)$. Thus, $\tilde{w}(\omega_A)$ and $\tilde{\Gamma}_A(\omega_A)$ can be viewed as measures of the energy-transfer rate and the donor-decay rate, respectively.

Figure 5 shows the dependence on d of $\tilde{\Gamma}_A(\omega_A)$ and $\tilde{w}(\omega_A)$ (averaged over the dipole orientations). From Fig. 5(a) it is seen that at $d/\lambda_A \sim 0.21$ (i.e., $d \sim 130$ nm for $\lambda_A = 614$ nm) the ratio of the donor-decay rates for the five- and four-layered systems is $\tilde{\Gamma}_A(\omega_A)|_5 / \tilde{\Gamma}_A(\omega_A)|_4 \sim 1.3$, which (within the measurement accuracy) is in sufficiently good agreement with experimental result (see Fig. 2D in Ref. [8]). Note that in the vicinity of $d/\lambda_A \sim 0.21$ the ratio of the two rates sensitively responds to a change of d/λ_A.

Comparing $\tilde{\Gamma}_A(\omega_A)$ [Fig. 5(a)] with $\tilde{w}(\omega_A)$ [Fig. 5(b)], we see that for the four-layered system and $d/\lambda_A \sim 0.16$–0.33 (i.e., $d \sim 100$–200 nm for $\lambda_A = 614$ nm) both $\tilde{\Gamma}_A(\omega_A)$ and $\tilde{w}(\omega_A)$ decrease with increasing d and an approximately valid linear relation between the energy-transfer rate and the donor-decay rate can be established, in agreement with experimental results in Ref. [8]. From the data reported in Ref. [8] it could be expected that the linear relation between the two rates is generally valid. This is of course not the case. Since the energy-transfer rate is determined by the full (two-point) Green tensor, whereas the donor-decay rate is only determined by the imaginary part of the (one-point) Green tensor, the two rates can behave quite differently, as it is demonstrated in Fig. 5. In particular, the increase of the donor-decay rate at the cavity resonances can be accompanied with a decrease of the energy-transfer rate, because of destructive interferences.

In the experiments in Ref. [8], the measurements are performed on an ensemble of donors and acceptors whose distance is fixed in the z direction but are variable in the x direction ($\Delta R_x \sim 1$ nm). The question thus arises of whether the measured data refer to a single nearest-neighboring donor-acceptor pair ($R_x = 0$) or not. In Fig. 6 we have plotted the dependence on d of $\tilde{w}(\omega_A)$ (averaged over the dipole orientations) for the five-layered system and various values of R_x, with R_z being fixed. We see that the rates of energy transfer between molecules whose distances are larger than those of nearest-neighboring molecules can be quite comparable with those of the latter. Moreover, there are also cases where the energy-transfer rate increases with the donor-acceptor distance. The experimentally determined energy-transfer rates are thus averaged rates, which do not necessarily show the characteristic features of single-pair transfer rates. Averaging in Fig. 6 $\tilde{w}(\omega_A)$ over all values of R_x, the resulting curve is expected to be substantially flatter than the solid-line curve ($R_x = 0$), particularly when d sweeps through λ_A.

An analysis of the contributions of $\boldsymbol{G}_1^{\rm refl}$ [Eq. (63)] and $\boldsymbol{G}_2^{\rm refl}$ [Eq. (64)] to $\boldsymbol{G}^{\rm refl}$ [Eq. (62)] reveals that for cavity lengths of $d/\lambda_A \lesssim 0.16$ (i.e., $d \lesssim 100$ nm for $\lambda_A = 614$ nm) evanescent waves dominate the influence of the cavity system on both the rate of intermolecular energy transfer and the donor-decay rate and lead to a strong increase in their values. Whereas for cavity lengths of $d/\lambda_A \gtrsim 0.81$ (i.e., $d \gtrsim 500$ nm for $\lambda_A = 614$ nm) evanescent waves only weakly affect the donor-decay rate, they can strongly affect the intermolecular

energy transfer up to cavity lengths of a few micrometers. Note that the resonance lengths seen in Fig. 5 originate from propagating waves.

C. Microsphere

Microspheres have been of increasing interest because of the whispering-gallery (WG) and surface-guided (SG) waves, which may be employed, e.g., for reducing the thresholds of nonlinear optical processes [28,29]. Intermolecular energy transfer in the presence of microspheres has been considered for molecules near a small metallic spheroid (spheroid's linear extension $\ll\lambda_A$) in the nonretardation limit, for molecules embedded within a dielectric microsphere [11,12], and for the case where one molecule is inside a dielectric microsphere and the other is outside it [13]. Here we restrict our attention to the influence of WG and SG waves on the energy transfer between two molecules outside a microsphere, taking fully into account retardation effects.

Let $\varepsilon_1(\omega)$ and $\varepsilon_2(\omega)$ be, respectively, the permittivities outside and inside the sphere. If the dipole-transition moments are parallel to each other and tangentially oriented with respect to the sphere, the relevant (spherical-coordinate) components of $\boldsymbol{G}^{\mathrm{refl}}$ are ($\phi_A=\phi_B=0,\ \theta_A=0$)

$$G^{\mathrm{refl}}_{\phi_B\phi_A}(\mathbf{r}_B,\mathbf{r}_A,\omega)=\frac{ik_1}{4\pi}\sum_{l=1}^{\infty}\frac{(2l+1)}{l(l+1)}\Big\{\mathcal{B}_l^M h_l^{(1)}(k_1r_A)h_l^{(1)}\times(k_1r_B)[l(l+1)P_l(\cos\theta_B)-\cos\theta_B P_l'(\cos\theta_B)]+\mathcal{B}_l^N\frac{[k_1r_A\,h_l^{(1)}(k_1r_A)]'}{k_1r_A}\times\frac{[k_1r_B\,h_l^{(1)}(k_1r_B)]'}{k_1r_B}P_l'(\cos\theta_B)\Big\} \tag{69}$$

(for the Green tensor of a sphere, see, e.g., [30]), and for radially oriented dipoles the relevant components are ($\phi_A=\phi_B=0,\ \theta_A=0$)

$$G^{\mathrm{refl}}_{r_Br_A}(\mathbf{r}_B,\mathbf{r}_A,\omega)=\frac{ik_1}{4\pi}\sum_{l=1}^{\infty}\frac{l(l+1)(2l+1)}{\overline{r_A}\,\overline{r_B}}\times\mathcal{B}_l^N h_l^{(1)}(k_1r_A)h_l^{(1)}(k_1r_B)P_l'(\cos\theta_B), \tag{70}$$

where

$$\mathcal{B}_l^M(\omega)=-\frac{[a_2j_l(a_2)]'j_l(a_1)-[a_1j_l(a_1)]'j_l(a_2)}{[a_2j_l(a_2)]'h_l^{(1)}(a_1)-j_l(a_2)[a_1h_l^{(1)}(a_1)]'}, \tag{71}$$

$$\mathcal{B}_l^N(\omega)=-\frac{\varepsilon_1(\omega)j_l(a_2)[a_1j_l(a_1)]'-\varepsilon_2(\omega)j_l(a_1)[a_2j_l(a_2)]'}{\varepsilon_1(\omega)j_l(a_2)[a_1h_l^{(1)}(a_1)]'-\varepsilon_2(\omega)[a_2j_l(a_2)]'h_l^{(1)}(a_1)} \tag{72}$$

[$a_{1,2}=k_{1,2}a$, a is the microsphere radius, $j_l(z)$ is the spherical Bessel function, $h_l^{(1)}(z)$ is the spherical Hankel function, $P_l^m(x)$ is the associated Legendre function].

In Fig. 7 the dependence on frequency of $\tilde{w}(\omega)$ is illustrated for the case where vacuum is outside the sphere and the two molecules are placed at diametrically opposite positions ($\mathbf{r}_A=-\mathbf{r}_B$), with the dipole-transition moments being radially oriented. It is clearly seen that the energy transfer can greatly be facilitated at the positions of the sphere-assisted field resonances, the enhancement of $\tilde{w}(\omega)$ at the positions of SG resonances (inside the band gap) being larger than those at the positions of WG resonances (outside the band gap). Maximum values of $\tilde{w}(\omega)$ are observed where the SG resonances overlap. The energy-transfer rate for tangentially oriented dipoles (not shown) is, in general, smaller than that for radially oriented dipoles. Note that when $\tilde{w}(\omega)$ is sharply peaked at the sphere-assisted field resonances, such that it is not slowly varying in the frequency interval where the (free-space) donor-emission and acceptor-absorption spectra overlap, then it cannot be taken at the electronic-energy-transfer frequency and put in front of the integral in Eq. (43). In this case, the change of the energy-transfer rate

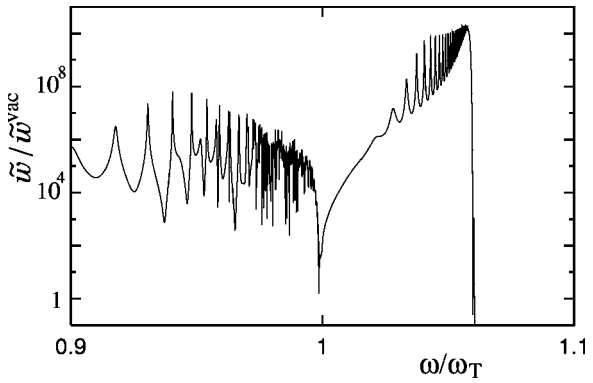

FIG. 7. The electronic part of the rate of energy transfer [Eq. (44)] between two molecules (at diametrically opposite positions) near a microsphere is shown as a function of frequency for radially oriented dipole-transition moments and a single-resonance Drude-Lorentz-type dielectric ($a=2\lambda_{\mathrm{T}}, r_A=r_B=2.02\lambda_{\mathrm{T}}, \omega_{\mathrm{P}}=0.5\omega_{\mathrm{T}}, \gamma/\omega_{\mathrm{T}}=10^{-4}$).

will be less pronounced than what might be expected from the frequency response of the electronic part, because of the frequency integration.

IV. CONCLUSIONS

We have given a rigorous, strictly quantum-mechanical derivation of the rate of intermolecular energy transfer in the presence of dispersing and absorbing material bodies of arbitrary shapes, showing that both the minimal-coupling scheme and the multipolar-coupling scheme lead to rate formulas of exactly the same form. The dependence on the material bodies of the energy-transfer rate is fully expressed in terms of the Green tensor of the macroscopic Maxwell equations for the medium-assisted electromagnetic field. In the macroscopic approach, the dispersing and absorbing material bodies are described, from the very beginning, in terms of a spatially varying permittivity, which is a complex function of frequency. The macroscopic approach has—similar to classical optics—the benefit of being universally valid, without the need of involved *ab initio* microscopic calculations. In sofar as such calculations for simple model systems have been performed, the results agree with those obtained from the microscopic approach. Clearly, macroscopic electrodynamics is valid only to some approximately fixed length scale, which exceeds the average interatomic distance in the material bodies.

Whereas the spontaneous donor- decay rate is determined by the imaginary part of the Green tensor in the coincidence limit, the donor-acceptor energy-transfer rate depends on the full two-point Green tensor. Hence, the decay rate and the energy-transfer rate can be affected by the presence of material bodies quite differently. Our calculations for planar multilayer structures have shown that enhancement (inhibition) of spontaneous decay and inhibition (enhancement) of energy transfer can appear simultaneously. They have further shown that surface-guided waves can strongly affect the energy transfer, thus being very suitable for controlling it.

In free space it is often distinguished between two limiting cases, namely, the short-distance nonradiative (Förster) energy transfer and the long-distance radiative energy transfer. The former is characterized by R^{-6} distance dependence of the transfer rate, and the latter by R^{-2} dependence. In particular, in the short-distance limit the energy-transfer rate rapidly decreases with increasing distance between the molecules. This must not necessarily be the case in the presence of material bodies, because of the possibly drastic change of the dependence on the distance of the energy-transfer rate. So, our calculations for planar multilayer structures have shown that the energy-transfer rate can also increase with the distance.

ACKNOWLEDGMENTS

We thank S. Scheel and A. Tip for discussions. H.T.D. is grateful to the Alexander von Humboldt Stiftung for financial support. This work was supported by the Deutsche Forschungsgemeinschaft.

APPENDIX A: DERIVATION OF THE TRANSFER RATE IN THE MULTIPOLAR-COUPLING SCHEME

The multipolar-coupling Hamiltonian can be obtained from the minimal-coupling Hamiltonian by means of the Power-Zienau transformation [3,4],

$$\hat{\mathcal{H}} = \hat{U}^{\dagger}\hat{H}\hat{U}, \tag{A1}$$

where

$$\hat{U} = \exp\left[\sum_M \frac{i}{\hbar}\int d^3\mathbf{r}\hat{\mathbf{P}}_M(\mathbf{r})\hat{\mathbf{A}}(\mathbf{r})\right] \tag{A2}$$

with

$$\hat{\mathbf{P}}_M(\mathbf{r}) = \sum_{\alpha_M} q_{\alpha_M}(\hat{\mathbf{r}}_{\alpha_M} - \mathbf{r}_M)\int_0^1 d\lambda\, \delta(\mathbf{r} - \mathbf{r}_M - \lambda(\hat{\mathbf{r}}_{\alpha_M} - \mathbf{r}_M)) \tag{A3}$$

being the polarization associated with the Mth molecule. Using $\hat{H}$ from Eq. (1), we derive (see, for details, [17])

$$\begin{aligned}\hat{\mathcal{H}} = &\int d^3\mathbf{r}\int_0^\infty d\omega\hbar\omega\hat{\mathbf{f}}^{\dagger}(\mathbf{r},\omega)\hat{\mathbf{f}}(\mathbf{r},\omega) + \sum_M\sum_{\alpha_M}\frac{1}{2m_{\alpha_M}}\\ &\times\left\{\hat{\mathbf{p}}_{\alpha_M} + q_{\alpha_M}\int_0^1 d\lambda\lambda(\hat{\mathbf{r}}_{\alpha_M} - \mathbf{r}_M)\times\hat{\mathbf{B}}[\mathbf{r}_M + \lambda\right.\\ &\left.\times(\hat{\mathbf{r}}_{\alpha_M} - \mathbf{r}_M)]\right\}^2 + \sum_M\int d^3\mathbf{r}\left[\frac{1}{2\varepsilon_0}\hat{\mathbf{P}}_M(\mathbf{r})\hat{\mathbf{P}}_M(\mathbf{r})\right]\\ &-\sum_M\int d^3\mathbf{r}[\hat{\mathbf{P}}_M(\mathbf{r})\hat{\mathbf{E}}(\mathbf{r})],\end{aligned} \tag{A4}$$

where $\hat{\mathbf{B}}(\mathbf{r}) = \boldsymbol{\nabla}\times\hat{\mathbf{A}}(\mathbf{r})$ [with $\hat{\mathbf{A}}(\mathbf{r})$ from Eq. (7)] and

$$\hat{\mathbf{E}}(\mathbf{r}) = \int_0^\infty d\omega\underline{\hat{\mathbf{E}}}(\mathbf{r},\omega) + \text{H.c.}, \tag{A5}$$

and neutral molecules with nonoverlapping charge distributions are again assumed. Note that in the multipolar-coupling scheme the operator of the electric-field strength is defined according to

$$\hat{\mathcal{E}}(\mathbf{r}) = -\frac{1}{i\hbar}[\hat{\mathbf{A}}(\mathbf{r}),\hat{\mathcal{H}}] - \boldsymbol{\nabla}\hat{\varphi}(\mathbf{r}) - \boldsymbol{\nabla}\hat{\phi}(\mathbf{r}), \tag{A6}$$

which implies the following relation between $\hat{\mathbf{E}}(\mathbf{r})$ and $\hat{\mathcal{E}}(\mathbf{r})$:

$$\varepsilon_0\hat{\mathbf{E}}(\mathbf{r}) = \varepsilon_0\hat{\mathcal{E}}(\mathbf{r}) + \sum_M\hat{\mathbf{P}}_M(\mathbf{r}). \tag{A7}$$

Hence, $\varepsilon_0\hat{\mathbf{E}}(\mathbf{r})$ has the meaning of the displacement field with respect to the molecular polarization.

From Eq. (A4) it is seen that the molecules now interact only via the medium-assisted electromagnetic field. In particular, in the (electric-) dipole approximation Eq. (A4) simplifies to

$$\hat{\mathcal{H}} = \hat{\mathcal{H}}_0 + \hat{\mathcal{H}}_{\rm int}, \tag{A8}$$

where

$$\hat{\mathcal{H}}_0 = \int d^3\mathbf{r} \int_0^\infty d\omega \hbar\omega\, \hat{\mathbf{f}}^\dagger(\mathbf{r},\omega)\hat{\mathbf{f}}(\mathbf{r},\omega) + \sum_M \hat{\mathcal{H}}_M \tag{A9}$$

with

$$\hat{\mathcal{H}}_M = \sum_{\alpha_M} \frac{1}{2m_{\alpha_M}} \hat{\mathbf{p}}^2_{\alpha_M} + \int d^3\mathbf{r} \frac{1}{2\varepsilon_0} \hat{\mathbf{P}}_M(\mathbf{r})\hat{\mathbf{P}}_M(\mathbf{r}) \tag{A10}$$

is the unperturbed Hamiltonian of the medium-assisted electromagnetic field and the molecules, and

$$\hat{\mathcal{H}}_{\rm int} = \sum_M \hat{\mathcal{H}}^{(M)}_{\rm int} = -\sum_M \hat{\mathbf{d}}_M \hat{\mathbf{E}}(\mathbf{r}_M) \tag{A11}$$

is the interaction energy between them.

Comparing the multipolar-coupling energy given by Eq. (A11) with the minimal-coupling energy $\hat{H}_{\rm int}$ given by Eq. (13) together with Eqs. (17)–(20), we see that the two energies (formally) become equal to each other, if we remove in the latter the Coulomb term and replace $-[\hat{\mathbf{d}}_M, \hat{\mathcal{H}}_M]/\hbar\omega$ with $\hat{\mathbf{d}}_M$. Having these changes in mind, we now follow step by step the derivation of Eq. (40) in Sec. II B. Starting from the corresponding eigenstates of the unperturbed multipolar-coupling Hamiltonian (instead of those of the unperturbed minimal-coupling Hamiltonian), it is not difficult to see that the result is again Eq. (40). It should be pointed out that the above-mentioned difference between $\hat{\mathbf{E}}(\mathbf{r})$ and $\hat{\mathcal{E}}(\mathbf{r})$ [Eq. (A7)] does not affect the energy-transfer rate.

APPENDIX B: SINGLE-MOLECULE EMISSION SPECTRUM

In the electric-dipole approximation and the rotating-wave approximation, the Hamiltonian for a single molecule (at position $\mathbf{r}_A$) that (with regard to the vibronic transitions $|a'\rangle \leftrightarrow |a\rangle$) resonantly interacts with the medium-assisted electromagnetic field reads, by appropriately specifying Eqs. (11)–(20) [18],

$$\hat{H} = \hat{H}_0 + \hat{H}_{\rm int}, \tag{B1}$$

$$\hat{H}_0 = \int d^3\mathbf{r} \int_0^\infty d\omega \hbar\omega\, \hat{\mathbf{f}}^\dagger(\mathbf{r},\omega)\hat{\mathbf{f}}(\mathbf{r},\omega) + \sum_a \hbar\omega_a |a\rangle \times \langle a| + \sum_{a'} \hbar\omega_{a'} |a'\rangle\langle a'|, \tag{B2}$$

$$\hat{H}_{\rm int} = -\sum_{a,a'} [|a'\rangle\langle a|\hat{\mathbf{E}}^{(+)}(\mathbf{r}_A)\mathbf{d}_{a'a} + {\rm H.c.}], \tag{B3}$$

where $\hat{\mathbf{E}}^{(+)}(\mathbf{r})$ is the positive-frequency part of $\hat{\mathbf{E}}(\mathbf{r})$ defined by Eq. (A5), and the vibronic-dipole-transition matrix elements $\mathbf{d}_{a'a}$ of the vibronic transitions are given, in the Born-Oppenheimer approximation, by Eq. (41). Let us assume that the molecule is initially (at time $t=0$) prepared in a statistical mixture of vibrational states in the upper electronic state and the medium-assisted electromagnetic field is in the vacuum state, i.e.,

$$\hat{\rho}(t=0) = \sum_{a'} p_{a'} |a'\rangle\langle a'| \otimes |\{0\}\rangle\langle\{0\}|. \tag{B4}$$

The time-dependent spectrum of light observed at position $\mathbf{r}$ (in free space) by means of a spectral apparatus of sufficiently small passband width can be given by (see, e.g., [31])

$$S(\mathbf{r},\omega_{\rm S},T) = \int_0^T dt_2 \int_0^T dt_1 [\exp\{-i\omega_{\rm S}(t_2-t_1)\} \times \langle \hat{\mathbf{E}}^{(-)}(\mathbf{r},t_2)\hat{\mathbf{E}}^{(+)}(\mathbf{r},t_1)\rangle], \tag{B5}$$

where $\omega_{\rm S}$ and T are, respectively, the setting frequency and the operating time of the spectral apparatus. In order to calculate the electric-field correlation function associated with the light emitted by the molecule during the spontaneous decay of the upper electronic state, we may restrict our attention to the perturbative expansion of the time-evolution operator up to the first order in $\hat{H}_{\rm int}$ [19],

$$e^{-i\hat{H}t/\hbar} \simeq e^{-i\hat{H}_0 t/\hbar} + \frac{1}{i\hbar}\int_0^t dt' \exp[-i\hat{H}_0(t-t')/\hbar] \times \hat{H}_{\rm int} e^{-i\hat{H}_0 t'/\hbar}. \tag{B6}$$

We make use of Eqs. (B3), (A5) [together with Eq. (9)], (B4), and (B6), apply Eq. (B5), and derive after some calculation, on recalling the relation (30) (see also [32]),

$$\lim_{T\to\infty} T^{-1} S(\mathbf{r},\omega_{\rm S},T) = 2\pi \sum_{a,a'} p_{a'} |v_{a'a}|^2 |\mathbf{F}(\mathbf{r},\mathbf{r}_A,\omega_{a'a})|^2 \times \delta(\omega_S - \omega_{a'a}), \tag{B7}$$

where

$$\mathbf{F}(\mathbf{r},\mathbf{r}_A,\omega_{a'a}) = \frac{1}{\pi\varepsilon_0}\int_0^\infty d\omega \frac{\omega^2}{c^2} {\rm Im}\, \boldsymbol{G}(\mathbf{r},\mathbf{r}_A,\omega)\mathbf{d}_A \zeta(\omega_{a'a}-\omega) \simeq -\frac{i\omega^2_{a'a}}{\varepsilon_0 c^2}\boldsymbol{G}(\mathbf{r},\mathbf{r}_A,\omega_{a'a})\mathbf{d}_A \tag{B8}$$

[$\zeta(x) = \pi\delta(x) + i{\rm P}(1/x)$; P is the principal value]. In the derivation of Eq. (B7), retardation has been ignored and the relation

$$\lim_{T\to\infty} \frac{1}{T}\int_0^T dt_2 \int_0^T dt_1 e^{-i\omega(t_2-t_1)} = \lim_{T\to\infty} \frac{\sin^2(\omega T/2)}{T(\omega/2)^2} = 2\pi\delta(\omega) \tag{B9}$$

has been used.

[1] *Resonance Energy Transfer*, edited by D. L. Andrews and A.A. Demidov (Wiley, New York, 1999).
[2] T. Förster, Ann. Phys. (Leipzig) **1**, 55 (1948); D.L. Dexter, J. Chem. Phys. **21**, 836 (1953).
[3] E.A. Power and S. Zienau, Philos. Trans. R. Soc. London, Ser. A **251**, 427 (1959); R.G. Woolley, Proc. R. Soc. London, Ser. A **321**, 557 (1971).
[4] D. P. Craig and T. Thirunamachandran, *Molecular Quantum Electrodynamics* (Academic, New York, 1984).
[5] J.S. Avery, Proc. Phys. Soc. London **88**, 1 (1966); L. Gomberoff and E.A. Power, *ibid.* **88**, 281 (1966); E.A. Power and T. Thirunamachandran, Phys. Rev. A **28**, 2671 (1983); D.L. Andrews and B.S. Sherborne, J. Chem. Phys. **86**, 4011 (1987); D.L. Andrews, Chem. Phys. **135**, 195 (1989); D.L. Andrews and G. Juzeliūnas, J. Chem. Phys. **96**, 6606 (1992); D.P. Craig and T. Thirunamachandran, Chem. Phys. **167**, 229 (1992).
[6] L.M. Folan, S. Arnold, and S.D. Druger, Chem. Phys. Lett. **118**, 322 (1985).
[7] M. Hopmeier, W. Guss, M. Deussen, E.O. Göbel, and R.F. Mahrt, Phys. Rev. Lett. **82**, 4118 (1999).
[8] P. Andrew and W.L. Barnes, Science **290**, 785 (2000).
[9] G. Juzeliūnas and D.L. Andrews, Phys. Rev. B **49**, 8751 (1994); **50**, 13 371 (1994).
[10] J.I. Gersten and A. Nitzan, Chem. Phys. Lett. **104**, 31 (1984).
[11] S.D. Druger, S. Arnold, and L.M. Folan, J. Chem. Phys. **87**, 2649 (1987).
[12] P.T. Leung and K. Young, J. Chem. Phys. **89**, 2894 (1988).
[13] V.V. Klimov and V.S. Letokhov, Phys. Rev. A **58**, 3235 (1998).
[14] T. Kobayashi, Q. Zheng, and T. Sekiguchi, Phys. Rev. A **52**, 2835 (1995); Phys. Lett. A **199**, 21 (1995).
[15] M. Cho and R.J. Silbey, Chem. Phys. Lett. **242**, 291 (1995).
[16] Ho Trung Dung, L. Knöll, and D.-G. Welsch, Phys. Rev. A **57**, 3931 (1998); S. Scheel, L. Knöll, and D.-G. Welsch, *ibid.* **58**, 700 (1998); A. Tip, L. Knöll, S. Scheel, and D.-G. Welsch, *ibid.* **63**, 043806 (2001).
[17] L. Knöll, S. Scheel, and D.-G. Welsch, in *Coherence and Statistics of Photons and Atoms*, edited by J. Peřina (Wiley, New York, 2001), p.1.
[18] S. Scheel, L. Knöll, and D.-G. Welsch, Phys. Rev. A **60**, 4094 (1999); Ho Trung Dung, L. Knöll, and D.-G. Welsch, *ibid.* **62**, 053804 (2000).
[19] C. Cohen-Tannoudji, J. Dupont-Roc, and G. Grynberg, *Atom-Photon Interactions* (Wiley, New York, 1992).
[20] V. May and O. Kühn, *Charge and Energy Transfer Dynamics in Molecular Systems* (Wiley-VCH, Berlin, 2000).
[21] M.S. Yeung and T.K. Gustafson, Phys. Rev. A **54**, 5227 (1996).
[22] M.S. Tomaš, Phys. Rev. A **51**, 2545 (1995).
[23] W. C. Chew, *Waves and Fields in Inhomogeneous Media* (IEEE Press, New York, 1995).
[24] S. Scheel, L. Knöll, and D.-G. Welsch, Acta Phys. Slov. **49**, 585 (1999).
[25] H. Raether, *Surface Plasmons on Smooth and Rough Surfaces and on Gratings* (Springer-Verlag, Berlin, 1988).
[26] P.T. Worthing, R.M. Amos, and W.L. Barnes, Phys. Rev. A **59**, 865 (1999).
[27] D.J. Nash and J.R. Sambles, J. Mod. Opt. **43**, 81 (1996).
[28] *Optical Processes in Microcavities*, edited by R. K. Chang and A. J. Campillo (World Scientific, Singapore, 1996).
[29] Ho Trung Dung, L. Knöll, and D.-G. Welsch, Phys. Rev. A **64**, 013804 (2001).
[30] L.W. Li, P.S. Kooi, M.S. Leong, and T.S. Yeo, IEEE Trans. Microwave Theory Tech. **42**, 2302 (1994).
[31] W. Vogel, D.-G. Welsch, and S. Wallentowitz, *Quantum Optics, An Introduction* (Wiley-VCH, Berlin, 2001).
[32] Ho Trung Dung, L. Knöll, and D.-G. Welsch, e-print quant-ph/0104056.